AGU ADVANCING EARTH AND SPACE SCIENCE

Geophysical Research Letters

RESEARCH LETTER
10.1029/2022GL099082

Key Points:

- Estuary length strongly affects tidal propagation, residual circulation, and salt intrusion in periodically weakly stratified estuaries
- The dominant salt balance may change when substantially reducing estuary length
- Steady lateral shear dispersion can reduce responses of salt intrusion to forcing changes in short estuaries with weak stratification

Supporting Information:

Supporting Information may be found in the online version of this article.

Correspondence to:

X. Wei,
xwei@noc.ac.uk

Citation:

Wei, X., Williams, M. E., Brown, J. M., Thorne, P. D., & Amoudry, L. O. (2022). Salt intrusion as a function of estuary length in periodically weakly stratified estuaries. *Geophysical Research Letters*, *49*, e2022GL099082. https://doi.org/10.1029/2022GL099082

Received 9 APR 2022
Accepted 13 JUL 2022

Salt Intrusion as a Function of Estuary Length in Periodically Weakly Stratified Estuaries

Xiaoyan Wei[1], Megan E. Williams[2], Jennifer M. Brown[1], Peter D. Thorne[1], and Laurent O. Amoudry[1]

[1]National Oceanography Centre, Liverpool, UK, [2]Departamento de Obras Civiles, Universidad Tecnica Federico Santa Maria, Valparaiso, Chile

Abstract Estuarine salt intrusion greatly threatens freshwater supply in surrounding lands. Physical barriers, which reduce the estuary length (L), are widely constructed to control salt intrusion. Yet, the role of L in salt intrusion remains unknown. Using a process-based, idealized, semi-analytical three-dimensional model, we systematically investigate for the first time this unknown for tide-dominated, periodically weakly stratified estuaries. Results show decreasing L significantly reduces salinities for short estuaries ($L < L_w/4$, with L_w the dominant tidal wavelength), but not for long estuaries. Tidal pumping remains a key salt importer in most estuaries, regardless of L. However, substantial decreases in L relative to $L_w/4$ can change the dominant landward salt importer from tidal pumping to horizontal diffusion. The latter, together with gravitational circulation, weakens responses of salt intrusion to changes in tidal and river forcing in short estuaries. This study highlights the importance of considering L to understanding and mitigating salt intrusion.

Plain Language Summary Salty seawater can enter rivers through estuaries, where rivers meet the sea, thus affecting the surrounding freshwater supply and the healthy functioning of estuarine ecosystems. To mitigate the adverse impact of salt intrusion under aggravating climate change and human activities, expensive salinity barriers are commonly built around the world. These barriers result in an abrupt change in the estuary length and can substantially affect estuarine salt intrusion. This study uses a simplified computer model to understand the dependency of salt intrusion on estuary length in estuaries with small top-to-bottom salinity differences. Our results show that estuary length substantially influences the salinity distribution and estuaries of different lengths can respond to changes in tides and river flow contrastingly. Our study highlights the importance of considering the impact of estuary length to effectively mitigate estuarine salt intrusion.

1. Introduction

Salt water can intrude rivers through estuaries and affect freshwater intake for domestic, agricultural, and industrial uses in surrounding lands. Estuarine salt intrusion also creates horizontal and vertical density gradients, which drive a residual current (i.e., gravitational circulation, GC) and determine density stratification. Hence, salt intrusion modifies the fate and transport path of other waterborne materials (e.g., sediment, nutrients, pollutants) and strongly affects the healthy functioning of estuarine ecosystems.

In recent decades, due to human activities (e.g., increasing upstream freshwater abstraction, channel deepening, sand mining) and climate change (e.g., extreme droughts, sea level rise), salt intrusion has been increasing in estuaries worldwide. Examples are the Pearl River and Yangtze estuaries, China (Ding et al., 2021; Gong & Shen, 2011), the Mekong Delta (Vietnam, Thailand, and Cambodia, see Smajgl et al., 2015), the Tagus estuary, Portugal (Rodrigues et al., 2019), the Hudson River estuary, USA (Ralston & Geyer, 2019), and the Mary River estuary, Australia (Miloshis & Valentine, 2013). Catastrophic salt intrusion in the Yangtze estuary threatened drinking water supply to around 25 million people for 23 days in 2014 (Zhu et al., 2020). The Mekong Delta, a critical region for food production (rice, shrimp), recorded its worst salt intrusion in the 2019/2020 dry season that caused a 6-month shortage of freshwater supply for the locals and threatened the global food security (IFRC, 2020).

To mitigate influences of salt intrusion and flooding, physical barriers (such as weirs and sluice gates) are widely built in estuaries (e.g., Jeong et al., 2010; Smajgl et al., 2015). These barriers need to be carefully designed because they are expensive and have adverse impacts on fish migration (Harris et al., 2016). They also result in an abrupt change in the distance between the mouth to the furthest upstream location of tidal influence (i.e., estuary

length, L). This length, also known as tidal intrusion length, strongly affects tidal propagation (Godin, 1991), residual circulation (Li & O'Donnell, 2005), sediment properties (Uncles et al., 2002), and sediment transport (Ridderinkhof et al., 2014). Since tidal and residual currents can both play an important role in salt transport (e.g., Lerczak et al., 2009; Wei et al., 2017), changes in L are likely to strongly affect estuarine salt intrusion (Chen et al., 2012). However, most studies have focused on responses of salt intrusion to the water depth, river discharge, and tidal amplitude (e.g., Lerczak et al., 2009; MacCready, 2004; Monismith et al., 2002; Prandle, 2004; Ralston et al., 2010), neglecting the effect of L. The fundamental role of L in salt dynamics remains poorly understood even though its importance to the residual (i.e., tidally averaged) salinity in central estuaries was theoretically derived decades ago (Chatwin, 1976). This blind spot means that designs for mitigation solutions currently implemented overlook the important role of L in affecting estuarine salt intrusion under increasing natural and anthropogenic stresses.

This paper aims to systematically investigate the role of L in affecting salt intrusion and its responses to changes in bathymetry and physical forcings. To that end, we applied the process-based, semi-analytical, three-dimensional model developed by Wei et al. (2021) to idealized, tidally dominated, periodically weakly stratified estuaries with different lengths and forcing/bathymetry conditions. Our results suggest that substantially changing L can induce a salt transport regime shift, which can result in contrasting responses of salt intrusion to forcing changes.

2. Research Methods

2.1. Model Description

This idealized model resolves the three-dimensional shallow water equations and salinity equation, assuming estuaries to be well mixed or periodically weakly stratified and the residual salinities do not change over time (i.e., equilibrium). The estuary mouth is forced by a prescribed surface elevation and residual salinity. A freshwater discharge is prescribed at the landward boundary where a barrier prevents tidal propagation and salt intrusion. The bed is impermeable, with a partial slip boundary condition (i.e., linearized bottom friction) applied at the top of the bottom logarithmic boundary layer. The depth-integrated tidal and salt fluxes are required to vanish at the landward and side boundaries.

The model allows the water motion and salinity at each of the dominant tidal and subtidal frequencies to be separately calculated using a semi-analytical approach detailed in Wei et al. (2021). It also allows an explicit dissection of physical processes that control salt intrusion, including tidal pumping, horizontal diffusion, and steady shear dispersion driven by residual circulation. Tidal pumping refers to the steady upstream salt flux due to temporal correlations between the tidal velocity and salinity, as defined by Simpson et al. (2001). This process is also known as tidal advective diffusion (Wei et al., 2016) and tidal oscillatory salt flux (Lerczak et al., 2006).

Residual circulation originates from

- horizontal salinity gradients and the associated baroclinic pressure gradients, also known as the density-driven circulation (Fischer et al., 1979) or GC. This definition is more complete than the classical estuarine circulation, which only considers two-dimensional GC and neglects lateral variations (Hansen & Rattray, 1965). In well-mixed or periodically weakly stratified estuaries, residual salinity, S_0, is vertically homogeneous. Hence, GC contributes to salt intrusion primarily through advecting the laterally varying S_0 by the laterally sheared residual circulation. Hereafter this contribution is called GC-induced steady lateral shear dispersion. This process is different from the steady vertical shear dispersion associated with vertical differences in S_0 and GC dominant in partially mixed estuaries (see, e.g., Monismith et al., 2002).
- temporal correlations between the vertical eddy viscosity and barotropic shear at the dominant tidal frequency, that is, the eddy viscosity-shear covariance (ESCO), which is called tidal ESCO circulation due to direct interactions by Dijkstra et al. (2017).
- advection of horizontal momentum by tidal currents (AC), also known as the tidal rectification processes (Huijts et al., 2009).
- tidal return flow and Stokes drift (TRFSD) due to temporal correlations between tidal surface elevation and velocity at the still water level.
- a steady shear at the still water level, which is at some distance from the free surface where the no-shear condition (NS) is applied.
- redistribution of the river discharge (RD).

The above definitions of "tidal pumping" and "advection" are different from Fischer et al. (1979), where they refer to the longitudinal dispersion due to tide-driven residual circulation and river-induced residual advection, respectively. Horizontal diffusion, DIFF, regroups and parameterizes unresolved diffusive and dispersive processes such as baroclinic/barotropic instabilities, horizontal mixing caused by complex bathymetry and geometry features, dynamic feedback of GC on the residual stratification and vertical eddy viscosity/diffusivity, and its impact on tides and ESCO (Dijkstra et al., 2017). Mathematical terms associated with the resolved processes can be found in Kumar et al. (2017) and Wei et al. (2021).

2.2. Experiment Design

Eight baseline experiments were conducted to explore the influence of L on salt intrusion, considering funnel-shaped estuaries with L decreasing from 200 to 25 km with a 25 km interval (expts. I–VIII, see Table S1 in Supporting Information S1). These experiments represent scenarios with a salinity barrier constructed at different locations along the estuary (Figure 1a). In all experiments, the estuary width B decreases exponentially landward,

$$B = B_m e^{-x/L_b}. \tag{1}$$

Here x is the longitudinal location, $B_m = 15$ km is the width at the mouth ($x = 0$), and $L_b = 42$ km is the convergence length. All estuaries have a channel-shoal structure with the thalweg depth decreasing landward (Figure 1b) as commonly found in natural estuaries. The water depth (H) is described by

$$H = H_1 + H_2\tilde{x} + H_3\,(1 - \tilde{x})\,e^{-C_s y^2}. \tag{2}$$

Here, $\tilde{x} = (x + L_e)\,/\,(L + L_e)$, with $L_e = 20$ km the extended length of the model domain for reducing numerical uncertainties (see notes of Table S1 in Supporting Information S1). $C_s = 8.38 \times 10^{-8}$ m^{-2} is a shoal parameter with larger C_s corresponding to narrower shoals and vice versa. $H_1 = 5$ m, $H_2 = 3$ m, and $H_3 = 10$ m are depth parameters. The thalweg depth at the mouth and head, as well as the minimum depth at the mouth remain the same across all experiments. The above bathymetry and geometry parameters were chosen such that all estuaries are medium wide (i.e., depth-to-width ratio $<1.5 \times 10^{-2}$) and weakly convergent, which allow strong residual circulations to be generated under periodically stratified conditions (Burchard et al., 2014; Schulz et al., 2015).

In these experiments, a semi-diurnal tidal amplitude ($A_{M_2} = 1.95$ m), a quarter-diurnal tidal amplitude ($A_{M_4} = 0.17$ m) with a relative phase of $-225.79°$ compared to the semi-diurnal tide, and a residual salinity ($S_0 = 31$ g/kg) are prescribed at the mouth. These parameters are representative of the Blackwater estuary (UK), following Wei et al. (2021). Tidal constituents at other frequencies can be included but are not included for simplicity. A constant river flow ($Q = 180$ m^3/s) and Coriolis parameter ($f = 10^{-4}$ rad/s, corresponding to latitude 45°N) are considered.

Following Wei et al. (2021), the vertical eddy viscosity (A_v) and vertical eddy diffusivity ($K_v = A_v$) are calculated from an empirical vertical mixing parameterization that dynamically depends on flow velocity, water depth, and salinity. For simplicity, the horizontal eddy viscosity and diffusivity (K_h) are assumed to linearly decrease with channel width,

$$K_h = K_{h_0} + C_h \frac{B}{B_m}, \tag{3}$$

with $K_{h_0} = 10$ m^2 s^{-1} and $C_h = 60$ m^2 s^{-1} for all experiments.

Six sensitivity experiments were conducted to explore the impact of L on the response of estuarine salt intrusion to channel dredging, sea level rise, spring-neap tidal variations, seasonal freshwater fluctuations, and upstream freshwater release. These experiments consider a 2-m increase in H (expts. IX, XII in Table S1 of Supporting Information S1), an increase in Q by a factor of 9 (expts. X, XIII), or a 50% reduction in A_{M_2} (expts. XI, XIV) for $L = 25$ km and $L = 200$ km, respectively. The other parameters, such as L_b and B_m, remain the same as those used in expts. I and VIII.

To illustrate the impact of channel width and shallow shoals on salt intrusion response to forcing changes in the short estuary, two experiments with width reduced by a factor of 3 (expts. XV, XVI) and two experiments with C_s reduced to 3.35×10^{-8} m^{-2} (expts. XVII, XVIII) are conducted for $Q = 180$ m^3/s and $Q = 1620$ m^3/s, respectively.

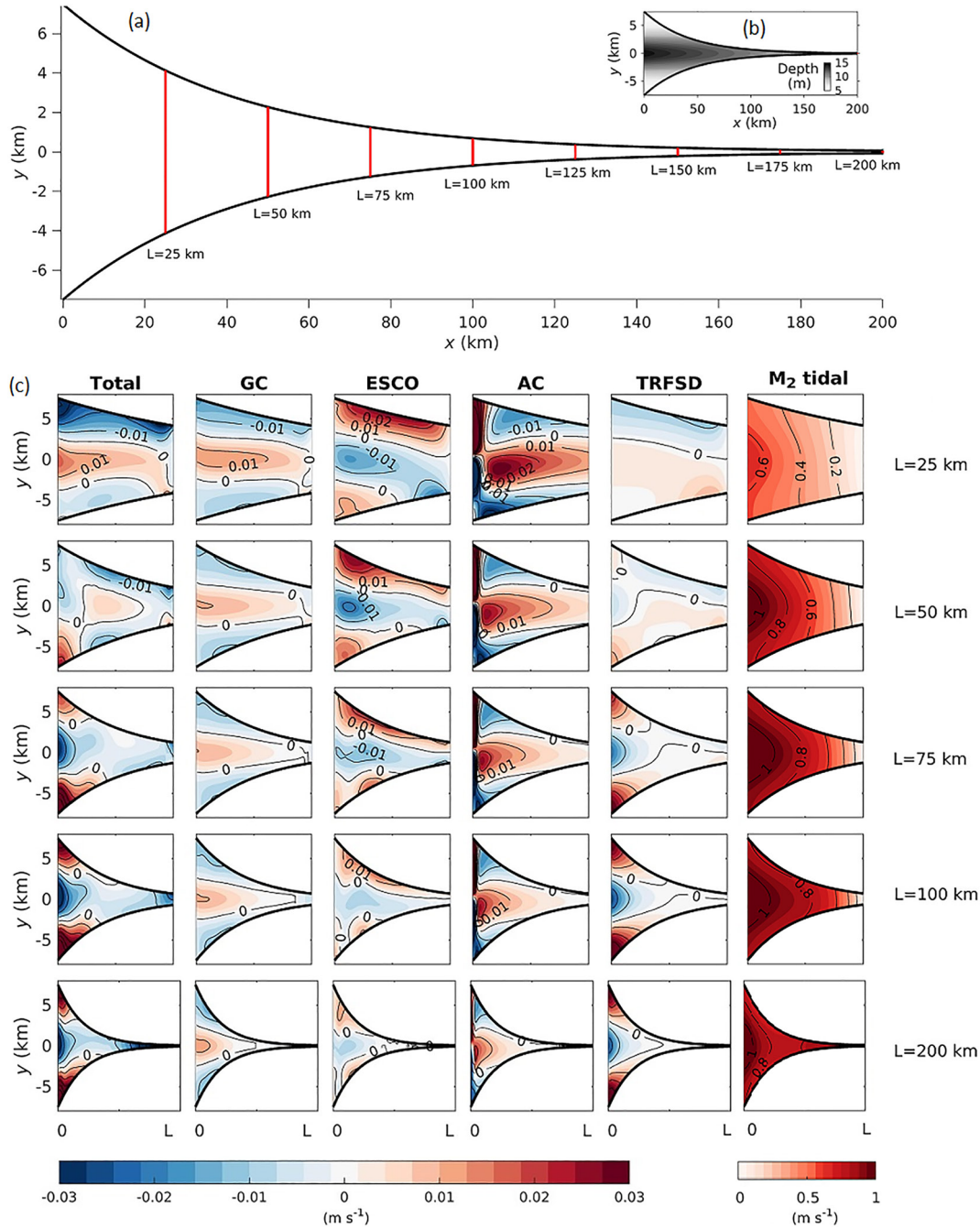

Figure 1. (a) Geometry of idealized estuaries with different lengths (L = 25:25:200 km). (b) Bathymetry of the longest idealized estuary with L = 200 km. (c) Along-channel component of the depth-averaged total residual circulation (first column), gravitational circulation (GC, second column), ESCO circulation (ESCO, third column), tidal advection-driven circulation (AC, fourth column), tidal return flow and Stokes drift (TRFSD, fifth column), and the depth-averaged semi-diurnal tidal velocity amplitude (last column) for L = 25, 50, 75, 100, and 200 km, respectively.

3. Influence of Estuary Length

3.1. Tidal and Residual Water Motion

The influence of L on the semi-diurnal tidal and residual currents, which can both transport salt into estuaries, is explored here. Since S_0 is vertically uniform, the residual salt transport due to residual circulation is associated with the depth-averaged lateral shear driven by each of the residual components and lateral salinity differences.

Figure 1c shows the depth-averaged total residual circulation, its four components (GC, ESCO, AC, and TRFSD), and the depth-averaged amplitude of the semi-diurnal tidal velocity in estuaries with L = 25, 50, 75, 100, and 200 km. Currents in estuaries with L = 125 – 175 km are similar to those with L = 200 km, hence are not presented. Results show a significant increase in the depth-averaged tidal velocity amplitude with increasing L for L < 100 km and a slight decrease with further increasing L for L > 100 km. This contrast is because 100 km is close to a quarter of the frictionless semi-diurnal (M_2) tidal wavelength (L_w/4), with

$$L_w = \sqrt{gH_m}T_w \tag{4}$$

(Le Blond, 1978) between 396 and 456 km for experiments I–VIII and T_w = 12.42 hr for the M_2 tidal period. This means, the estuary with L = 100 km is in approximate quarter-wave resonance with the M_2 tide despite moderate bottom friction, in accordance with Schuttelaars and De Swart (2000). Increasing L in short estuaries (with $L < L_w/4$) significantly enhances tidal currents as the semi-diurnal tide propagates more like a progressive wave (rather than a standing wave). For long estuaries (with $L > L_w/4$), however, increasing L results in strong tidal damping in the lower reach.

In all experiments, both GC and AC show an inflow through the channel and outflow over the shoals, whereas ESCO and TRFSD show an opposite structure: inflow over the shoals and outflow through the channel. The total residual circulation shows a similar depth-averaged structure to GC for L = 25 km, and a reversed pattern for $L \geq 75$ km. This is because AC and GC dominate the residual circulation for L = 25 km, whereas the sum of TRFSD and ESCO is stronger than the sum of AC and GC for $L \geq 75$ km. For L = 50 km, the total residual circulation shows contrasting structures between the lower reach and the middle reach. This is due to the residual circulation being dominated by ESCO in the lower reach and AC in the middle. The shift in the residual circulation pattern from the lower reach to the middle reach of a medium-sized estuary is consistent with observations in the Winyah Bay (Kim & Voulgaris, 2005).

3.2. Salinity Distribution

Changes in L have a clear impact on S_0, the main constituent of the total salinity. In short estuaries ($L < L_w/4$), salt intrusion retreats seaward substantially with decreasing L (Figure 2a). However, for $L > L_w/4$, salt intrusion only slightly decreases with decreasing L. Due to Coriolis effects and the channel-shoal structure, S_0 shows clear lateral variability at x = 20 km in all experiments (Figure 2b), measured by the lateral residual salinity anomaly defined as deviations from the laterally averaged S_0. The lateral residual salinity anomaly does not monotonically change with L but the largest anomaly is found in the shortest estuary (L = 25 km).

3.3. Residual Salt Balance

The influence of L on the residual salt balance is evaluated by comparing the cross-sectionally integrated longitudinal salt transport (T_s) due to each process for the short and long estuary (L = 25, 200 km), respectively. Remarkable differences in residual salt balance are found between these estuaries. For L = 25 km, DIFF is the dominant salt import process (Figure 2c, pink line), followed by TASF (red line). Lateral shear dispersion driven by GC (black line), AC (orange line), NS (yellow line), and TRFSD (brown line) also play a non-negligible role in transporting salt landward. River flushing (RD, gray line) dominates the seaward salt transport, followed by ESCO circulation (blue line). For L = 200 km, DIFF dominates the landward salt transport near the mouth but is smaller than TASF in most of the salt intrusion region (Figure 2d). Salt transport due to all residual circulation components (except RD) are negligible. The dominance of TASF and DIFF in residual salt transport in estuaries under strong tidal influences is consistent with Dijkstra and Schuttelaars (2021), where TASF is unresolved but parameterized as DIFF.

3.4. Dominant Salt Transport Processes

The role of L in estuarine salt intrusion is further investigated by comparing contributions of four important salt transport processes in all estuaries of different lengths. Figure 2e shows the ratio of the longitudinal salt transport due to TASF (R_{TASF}, red lines), GC (R_{GC}, black lines), and ESCO (R_{ESCO}, blue lines) to the DIFF-induced transport. Decreasing L results in a monotonically decreasing R_{TASF} within the salt intrusion region. This is due

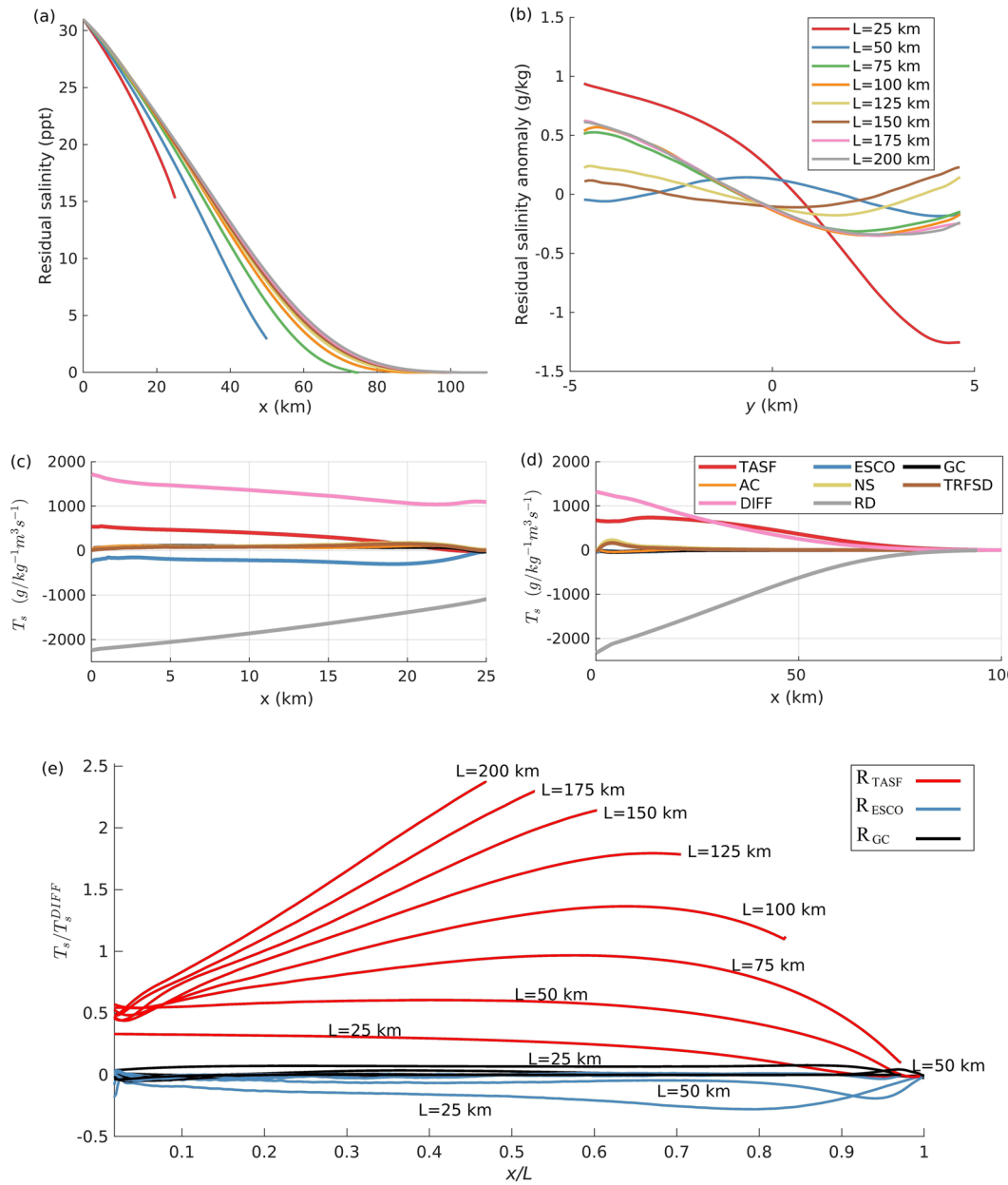

Figure 2. (a) Along-channel distribution of the width-averaged residual salinity and (b) cross-channel distribution of lateral residual salinity anomaly at $x = 20$ km for $L = 25{:}25{:}200$ km (expts. I–VIII). (c and d) Cross-sectionally integrated longitudinal, residual salt transport T_s due to tidal pumping (TASF), ESCO circulation (ESCO), gravitational circulation (GC), tidal advection (AC), no-shear surface condition (NS), tidal return flow compensating Stokes drift (TRFSD), horizontal diffusion (DIFF), and river discharge (RD) for $L = 25$ km (left panel) and $L = 200$ km (right panel). (e) Ratio of T_s due to TASF (R_{TASF}), GC (R_{GC}), and ESCO (R_{ESCO}) to the DIFF-induced transport, T_s^{DIFF}. Positive ratios mean landward transport and vice versa. Discontinuities of ratios at $x/L \sim 0.02$ are associated with sharp velocity and salinity gradients generated on the shoals to satisfy the closed side and open boundary conditions.

to relatively small K_h values in the lower reach and strong tidal currents in the upper reach of long estuaries compared to short ones (Figure 1, last column). For long estuaries ($L > L_w/4$), TASF dominates salt import ($R_{TASF} > 1 > R_{GC}$) in the middle/upper reaches. For short estuaries ($L < L_w/4$), DIFF becomes dominant and TASF is the second ($R_{GC} < R_{TASF} < 1$). The strong dependence of TASF on L can be explained as its magnitude scales approximately with the tidal surface gradients squared (Wei et al., 2016). These gradients are controlled by tidal propagation characteristics which differ greatly between short and long estuaries (Figure 1). R_{GC} remains close to

0 for $L > L_w/4$. It exceeds R_{TASF} in the upper estuary for $L = 25$, 50 km, but remains less than 1 in all experiments. These results suggest a possible salt transport regime shift (i.e., from TASF-dominated to DIFF-dominated regime) by substantially changing L in estuaries under strong tidal influences and limited salinity stratification.

4. Responses to Changing Bathymetry, Tidal, and River Forcings

4.1. Sensitivity to Water Depth

Figures 3a and 3b show the along-channel distribution of the width-averaged S_0 and cross-channel distribution of lateral residual salinity anomaly in the shortest (red lines) and longest (gray lines) estuaries ($L = 25$, 200 km) with increased H (dotted lines), increased Q (dashed lines), and reduced tides (dash-dotted lines). Hereafter, the two estuaries are referred to as the long estuary and the short estuary, respectively. Increasing H by 2 m results in an increased S_0 in both estuaries, but almost has no impact on the lateral residual salinity anomaly at $x = 20$ km in the long estuary (Figure 3b, comparing dotted lines with solid lines which show the baseline results). However, the lateral salinity anomaly is increased by up to ∼0.5 g/kg in the short estuary (Figure 3b, red dotted lines).

Figures 3c and 3d show the ratio of the landward transport induced by TASF, GC, and ESCO to the DIFF-induced transport: R_{TASF} (red lines), R_{GC} (black lines), and R_{ESCO} (blues lines). For $L = 25$ km, deepening slightly increases R_{TASF} in the lower estuary and decreases it in the upper estuary (see dotted and solid red lines). This is because the increased depth results in a reduced longitudinal salinity gradient and modifies tidal advective diffusivity (Wei et al., 2016), while the prescribed K_h is unchanged. Meanwhile, deepening increases the magnitude of R_{GC} and R_{ESCO} throughout the estuary due to strengthened residual circulation and increased lateral residual salinity anomaly (Figure 3b). Consequently, GC becomes more important than TASF for $x/L > 0.8$ (black and red dotted lines, Figure 3c). For $L = 200$ km, deepening increases R_{TASF} and enhances the dominant role of TASF in salt intrusion, but it does not affect the negligible salt transport of GC or ESCO. Assuming processes parameterized by K_h do not change with depth, the above results imply that after deepening or sea level rise, salt intrusion is likely to depend less on tides in the short estuary but more strongly in the long estuary.

4.2. Sensitivity to River Discharge

Increasing Q by a factor of 9 significantly reduces S_0 in both estuaries, comparing solid and dashed lines in Figure 3a. In the long estuary, the salt intrusion length (L_s) is reduced by ∼50 km due to increased Q. Here, L_s is defined as the distance from the mouth to the location where the width-averaged S_0 reaches 1 g/kg, with $L_s = L$ in the case of $S_0 > 1$ g/kg at $x = L$. In the short estuary, increasing Q reduces L_s by ∼5 km and enlarges the lateral salinity anomalies (Figure 3b, dashed red line). It also completely changes the cross-channel distribution of lateral salinity anomaly in the long estuary (dashed gray line). Decreasing Q increases S_0 in both experiments, but L_s remains equal to L in the short estuary as found in the short estuary with default forcings (not shown).

Increasing Q strongly affects the residual salt balance in both estuaries. For $L = 200$ km, it results in an ESCO-induced landward salt transport in the upper region of salt intrusion and an increased R_{GC} due to strengthened GC and increased lateral salinity anomaly. Meanwhile, R_{TASF} is reduced within most of the salt intrusion region due to increased longitudinal salinity gradients and DIFF. For $L = 25$ km, increasing Q slightly reduces R_{TASF} due to increased DIFF. Meanwhile, it significantly increases R_{GC} as a result of strengthened GC and increased lateral salinity anomalies. The contribution of GC becomes almost as important as DIFF at $x/L \sim 0.2$.

4.3. Sensitivity to Tides

For $L = 25$ km, reducing the tidal forcing almost has no impact on S_0 (comparing solid and dash-dotted red lines, Figure 3a). Nevertheless, it increases the lateral salinity anomaly (Figure 3b, dash-dotted red line), similar to the effects of increasing Q. For $L = 200$ km, reduced tides results in a 20 km retreat of L_s (Figure 3a). Halving the tides reduces the relative importance of TASF and ESCO to salt transport and increases that of GC in both estuaries (Figures 3c and 3d). This effect is more pronounced in the short estuary, where GC overtakes TASF and becomes the second most important salt importer.

The importance of DIFF in experiments with small L_s may be related to strong longitudinal salinity gradients (as DIFF is proportional to these gradients), underestimated GC-induced steady vertical shear dispersion restricted

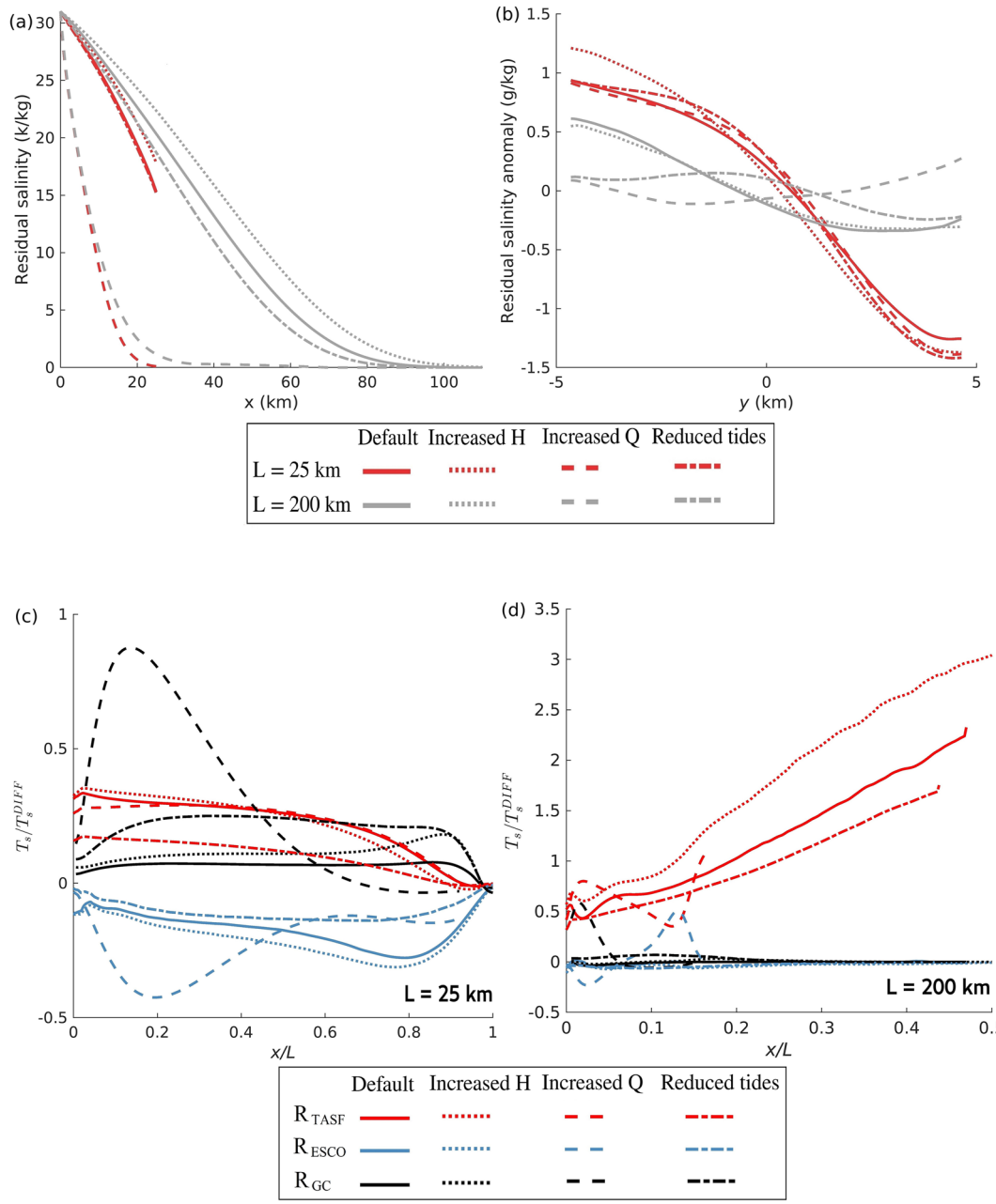

Figure 3. (a and b) Similar to Figures 2a and 2b but for sensitivity experiments with increased H (dotted lines), increased Q (dashed lines), or reduced tidal forcing (dash-dotted lines) for $L = 25$ km (red lines) and 200 km (gray lines), respectively. Solid lines show the baseline results with default bathymetry and forcings. (c and d) Similar to Figure 2e but for the above-mentioned sensitivity experiments.

by the model assumption of weak stratification and strong vertical mixing, and potentially important but unresolved mixing effects of complex geometry and bathymetry.

4.4. Implications of Salt Transport Regime Shift for Salt Intrusion

Results above show that salt intrusion in the long estuary is more sensitive to changes in tidal and/or river forcing compared to that in the short estuary. This can be explained by the different salt transport regimes in the two estuaries. In the long estuary, TASF makes the largest contribution to balancing the river-induced seaward salt transport. Since TASF is almost proportional to tidal surface gradients squared (Wei et al., 2016), halving the

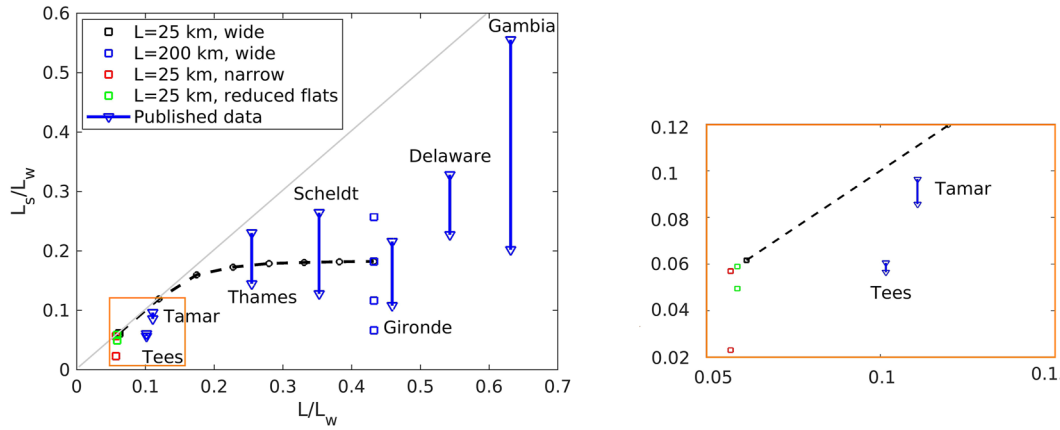

Figure 4. Estuary length (L) versus salt intrusion length (L_s) non-dimensionalized by the semi-diurnal tidal wavelength (L_w) for L = 25:25:200 km (expts. I–VIII, black circles with dashed line). Black and blue squares show L_s/L_w with Q = 60, 180, 540, 1620 m^3/s for L = 25 km (expt. I) and L = 200 km (expt. VIII), respectively. Red and green squares show results for the short estuary with a narrow channel and reduced flats, respectively. Blue triangles show maximum (upper triangles) and minimum (lower triangles) L_s/L_w versus L/L_w of natural estuaries. The gray line marks $L_s = L$. The right panel is a zoomed-in version of the orange box in the left panel.

tidal forcing significantly reduces TASF and results in a remarkably weakened salt intrusion. In the short estuary, reducing tidal forcing or increased Q tends to weaken salt intrusion and increase longitudinal salinity gradients. These gradients in turn promote contributions of DIFF and GC, compensate the reduced TASF-induced salt import and increased RD-induced salt export, therefore reducing the responses of salt intrusion to forcing changes.

5. Discussion

5.1. Impact of Estuary Width and Bathymetry

Even though GC-induced lateral shear dispersion is not the dominant salt transport process in any of the experiments considered here, it is largely responsible for the weak responses of L_s to forcing changes in the short estuary. The importance of this lateral shear dispersion to salt transport confirms findings of Fischer (1972) and Smith (1977), but remains largely overlooked in literature.

In addition to L, GC-induced lateral shear dispersion also depends on estuary geometry and bathymetry, particularly the channel width and lateral depth profile. Narrowing the estuary by a factor of 3 substantially reduced the lateral shear dispersion, as observed in the Tamar estuary (Uncles et al., 1985), and results in a remarkably smaller L_s when increasing Q (expts. XV–XVI, see red squares in Figure 4). Similarly, GC is weakened by reducing lateral depth differences (e.g., with deeper shoals), and L_s becomes more sensitive to Q (green squares) compared to the default short estuary (black squares). The importance of lateral shear dispersion has also been observed in narrow estuaries, such as the Tees (Lewis, 1979) and the Mersey estuary (Fischer, 1972), probably due to their deep channel and large intertidal areas which promote lateral shear dispersion.

5.2. Comparison to Realistic Estuaries

To understand the impact of L on salt intrusion in natural estuaries, the response of L_s to Q are explored for estuaries with different L, including the Tees and Thames (UK), Gironde (France), Scheldt (Netherlands, Belgium), Delaware (USA), and Gambia (Gambia) estuaries. Here, L and L_s are non-dimensionalized by the semi-diurnal tidal wavelength (L_w, see Equation 4). Values of L, L_s, and L_w of these estuaries are extracted or estimated from published data (see Table S2 in Supporting Information S1 for details).

Figure 4 shows L_s/L_w versus L/L_w in the baseline experiments (black dashed line with circles), sensitivity experiments with different Q for L = 25 km (black squares) and L = 200 km (blue squares), and natural estuaries with variable forcings (blue triangles). Due to geometrical, bathymetrical, and forcing differences between idealized

and natural estuaries, the simulated L_s generally deviates from that in natural estuaries with similar L. Nevertheless, in both natural and idealized estuaries, L_s is closer to and more constrained by L in short estuaries (Tees, Tamar) than in long ones. As a result, L_s responds to fluctuations of Q more weakly in shorter estuaries for both idealized and natural estuaries with one major channel. For example, L_s only slightly changes with Q in the Tees estuary (Bassindale, 1943), but changes by more than half of its length in the Gambia estuary (Albaret et al., 2004). This trend does not apply to the Gironde or the Delaware estuary, which may be due to more than one main tributaries in the lower Gironde estuary (Masson et al., 2009) and transitions from well-mixed to partially mixed conditions in the Delaware estuary (Geyer et al., 2020).

Unlike well-mixed or weakly stratified estuaries, weak response of L_s to forcing changes in the (partially mixed) Tamar estuary is due to combined effects of tidal pumping, lateral shear dispersion, and vertical shear dispersion (Uncles et al., 1985). Due to the weakly stratified assumption, the idealized model significantly underestimates the contribution of vertical shear dispersion in the case of strong stratification. To better understand the influence of L on salt intrusion in estuaries which can become partially mixed or strongly stratified, numerical models that resolve the feedback between vertical and lateral processes, as well as tidal processes, can be used but is out of scope of this study.

6. Conclusions

This study systematically investigates the role of estuary length (L) in salt intrusion in tidally dominated estuaries with weak stratification. Results show L affects not only the tidal currents, residual circulation, but also the estuarine salt intrusion. In estuaries under moderate river flow and strong tidal forcing, tidal pumping and horizontal diffusion are dominant salt transport processes. In short estuaries, lateral shear dispersion due to GC can also be important and strongly affect the response of salt intrusion to forcing changes. Our study highlights the necessity of considering the impact of changes in L when planning and designing estuarine barrier constructions to control salt intrusion and flooding.

Data Availability Statement

Model outputs of this study are available at: https://doi.org/10.5281/zenodo.5500232.

Acknowledgments
This work is funded by the NERC BLUE-coast project (NE/N015894/1, NE/N015894/2) and CHAMFER project (NE/W004992/1). LOA also acknowledges funding by EPSRC (Newton Fund) to the SUPREME project (EP/R024480/2). MEW acknowledges funding from ANID Fondecyt 11191077. We appreciate constructive comments from Yoeri Dijkstra and an anonymous reviewer which helped to improve the paper.

References

Albaret, J.-J., Simier, M., Darboe, F. S., Ecoutin, J.-M., Raffray, J., & de Morais, L. T. (2004). Fish diversity and distribution in the Gambia estuary, west Africa, in relation to environmental variables. *Aquatic Living Resources*, *17*(1), 35–46. https://doi.org/10.1051/alr:2004001

Bassindale, R. (1943). A comparison of the varying salinity conditions of the Tees and Severn estuaries. *Journal of Animal Ecology*, *12*, 1–10. https://doi.org/10.2307/1407

Burchard, H., Schulz, E., & Schuttelaars, H. M. (2014). Impact of estuarine convergence on residual circulation in tidally energetic estuaries and inlets. *Geophysical Research Letters*, *41*(3), 913–919. https://doi.org/10.1002/2013gl058494

Chatwin, P. (1976). Some remarks on the maintenance of the salinity distribution in estuaries. *Estuarine and Coastal Marine Science*, *4*(5), 555–566. https://doi.org/10.1016/0302-3524(76)90030-x

Chen, S.-N., Geyer, W. R., Ralston, D. K., & Lerczak, J. A. (2012). Estuarine exchange flow quantified with isohaline coordinates: Contrasting long and short estuaries. *Journal of Physical Oceanography*, *42*(5), 748–763. https://doi.org/10.1175/jpo-d-11-086.1

Dijkstra, Y. M., & Schuttelaars, H. M. (2021). A unifying approach to subtidal salt intrusion modeling in tidal estuaries. *Journal of Physical Oceanography*, *51*(1), 147–167. https://doi.org/10.1175/jpo-d-20-0006.1

Dijkstra, Y. M., Schuttelaars, H. M., & Burchard, H. (2017). Generation of exchange flows in estuaries by tidal and gravitational eddy viscosity-shear covariance (ESCO). *Journal of Geophysical Research: Oceans*, *122*(5), 4217–4237. https://doi.org/10.1002/2016jc012379

Ding, Z., Zhu, J., & Lyu, H. (2021). Impacts of the Qingcaosha Reservoir on saltwater intrusion in the Changjiang estuary. *Anthropocene Coasts*, *4*(1), 17–35. https://doi.org/10.1139/anc-2020-0015

Fischer, H. (1972). Mass transport mechanisms in partially stratified estuaries. *Journal of Fluid Mechanics*, *53*(4), 671–687. https://doi.org/10.1017/s0022112072000412

Fischer, H., List, J. E., Koh, C. R., Imberger, J., & Brooks, N. H. (1979). *Mixing in inland and coastal waters*. Academic Press.

Geyer, W. R., Ralston, D. K., & Chen, J.-L. (2020). Mechanisms of exchange flow in an estuary with a narrow, deep channel and wide, shallow shoals. *Journal of Geophysical Research: Oceans*, *125*, e2020JC016092. https://doi.org/10.1029/2020jc016092

Godin, G. (1991). Frictional effects in river tides. *Tidal Hydrodynamics*, *379*, 402.

Gong, W., & Shen, J. (2011). The response of salt intrusion to changes in river discharge and tidal mixing during the dry season in the Modaomen estuary, China. *Continental Shelf Research*, *31*(7–8), 769–788. https://doi.org/10.1016/j.csr.2011.01.011

Hansen, D. V., & Rattray, M., Jr. (1965). Gravitational circulation in straits and estuaries. *Journal of Marine Research*, *23*(2), 104–122.

Harris, J., Kingsford, R., Peirson, W., & Baumgartner, L. (2016). Mitigating the effects of barriers to freshwater fish migrations: The Australian experience. *Marine and Freshwater Research*, *68*(4), 614–628. https://doi.org/10.1071/MF15284

Huijts, K., Schuttelaars, H., De Swart, H., & Friedrichs, C. (2009). Analytical study of the transverse distribution of along-channel and transverse residual flows in tidal estuaries. *Continental Shelf Research*, *29*(1), 89–100. https://doi.org/10.1016/j.csr.2007.09.007

IFRC. (2020). Viet Nam: Drought and saltwater intrusion.
Jeong, S., Yeon, K., Hur, Y., & Oh, K. (2010). Salinity intrusion characteristics analysis using EFDC model in the downstream of Geum River. *Journal of Environmental Sciences*, *22*(6), 934–939. https://doi.org/10.1016/s1001-0742(09)60201-1
Kim, Y. H., & Voulgaris, G. (2005). Effect of channel bifurcation on residual estuarine circulation: Winyah Bay, South Carolina. *Estuarine, Coastal and Shelf Science*, *65*(4), 671–686. https://doi.org/10.1016/j.ecss.2005.07.004
Kumar, M., Schuttelaars, H. M., & Roos, P. C. (2017). Three-dimensional semi-idealized model for estuarine turbidity maxima in tidally dominated estuaries. *Ocean Modelling*, *113*, 1–21. https://doi.org/10.1016/j.ocemod.2017.03.005
Le Blond, P. H. (1978). On tidal propagation in shallow rivers. *Journal of Geophysical Research*, *83*(C9), 4717–4721. https://doi.org/10.1029/jc083ic09p04717
Lerczak, J. A., Geyer, W. R., & Chant, R. J. (2006). Mechanisms driving the time-dependent salt flux in a partially stratified estuary. *Journal of Physical Oceanography*, *36*(12), 2296–2311. https://doi.org/10.1175/jpo2959.1
Lerczak, J. A., Geyer, W. R., & Ralston, D. K. (2009). The temporal response of the length of a partially stratified estuary to changes in river flow and tidal amplitude. *Journal of Physical Oceanography*, *39*(4), 915–933. https://doi.org/10.1175/2008jpo3933.1
Lewis, R. (1979). Transverse velocity and salinity variations in the Tees estuary. *Estuarine and Coastal Marine Science*, *8*(4), 317–326. https://doi.org/10.1016/0302-3524(79)90049-5
Li, C., & O'Donnell, J. (2005). The effect of channel length on the residual circulation in tidally dominated channels. *Journal of Physical Oceanography*, *35*(10), 1826–1840. https://doi.org/10.1175/jpo2804.1
MacCready, P. (2004). Toward a unified theory of tidally-averaged estuarine salinity structure. *Estuaries*, *27*(4), 561–570. https://doi.org/10.1007/bf02907644
Masson, M., Schäfer, J., Blanc, G., Dabrin, A., Castelle, S., & Lavaux, G. (2009). Behavior of arsenic and antimony in the surface freshwater reaches of a highly turbid estuary, the Gironde estuary, France. *Applied Geochemistry*, *24*(9), 1747–1756. https://doi.org/10.1016/j.apgeochem.2009.05.004
Miloshis, M., & Valentine, E. (2013). Sea level rise and potential mitigation of saline intrusion in Northern Australia. In *2013 IAHR Congress* (pp. 9158–9167).
Monismith, S. G., Kimmerer, W., Burau, J. R., & Stacey, M. T. (2002). Structure and flow-induced variability of the subtidal salinity field in northern San Francisco Bay. *Journal of Physical Oceanography*, *32*(11), 3003–3019. https://doi.org/10.1175/1520-0485(2002)032<3003:safivo>2.0.co;2
Prandle, D. (2004). Saline intrusion in partially mixed estuaries. *Estuarine, Coastal and Shelf Science*, *59*(3), 385–397. https://doi.org/10.1016/j.ecss.2003.10.001
Ralston, D. K., & Geyer, W. R. (2019). Response to channel deepening of the salinity intrusion, estuarine circulation, and stratification in an urbanized estuary. *Journal of Geophysical Research: Oceans*, *124*(7), 4784–4802. https://doi.org/10.1029/2019jc015006
Ralston, D. K., Geyer, W. R., & Lerczak, J. A. (2010). Structure, variability, and salt flux in a strongly forced salt wedge estuary. *Journal of Geophysical Research: Oceans*, *115*(C6). https://doi.org/10.1029/2009jc005806
Ridderinkhof, W., De Swart, H., Van Der Vegt, M., Alebregtse, N., & Hoekstra, P. (2014). Geometry of tidal inlet systems: A key factor for the net sediment transport in tidal inlets. *Journal of Geophysical Research: Oceans*, *119*(10), 6988–7006. https://doi.org/10.1002/2014jc010226
Rodrigues, M., Fortunato, A. B., & Freire, P. (2019). Saltwater intrusion in the upper Tagus estuary during droughts. *Geosciences*, *9*(9), 400. https://doi.org/10.3390/geosciences9090400
Schulz, E., Schuttelaars, H. M., Gräwe, U., & Burchard, H. (2015). Impact of the depth-to-width ratio of periodically stratified tidal channels on the estuarine circulation. *Journal of Physical Oceanography*, *45*(8), 2048–2069. https://doi.org/10.1175/jpo-d-14-0084.1
Schuttelaars, H., & De Swart, H. (2000). Multiple morphodynamic equilibria in tidal embayments. *Journal of Geophysical Research*, *105*(C10), 24105–24118. https://doi.org/10.1029/2000jc900110
Simpson, J. H., Vennell, R., & Souza, A. J. (2001). The salt fluxes in a tidally-energetic estuary. *Estuarine, Coastal and Shelf Science*, *52*(1), 131–142. https://doi.org/10.1006/ecss.2000.0733
Smajgl, A., Toan, T. Q., Nhan, D. K., Ward, J., Trung, N. H., Tri, L., et al. (2015). Responding to rising sea levels in the Mekong Delta. *Nature Climate Change*, *5*(2), 167–174. https://doi.org/10.1038/nclimate2469
Smith, R. (1977). Long-term dispersion of contaminants in small estuaries. *Journal of Fluid Mechanics*, *82*(1), 129–146. https://doi.org/10.1017/s0022112077000561
Uncles, R., Elliott, R., & Weston, S. (1985). Dispersion of salt and suspended sediment in a partly mixed estuary. *Estuaries*, *8*(3), 256–269. https://doi.org/10.2307/1351486
Uncles, R., Stephens, J., & Smith, R. (2002). The dependence of estuarine turbidity on tidal intrusion length, tidal range and residence time. *Continental Shelf Research*, *22*(11–13), 1835–1856. https://doi.org/10.1016/s0278-4343(02)00041-9
Wei, X., Kumar, M., & Schuttelaars, H. M. (2017). Three-dimensional salt dynamics in well-mixed estuaries: Influence of estuarine convergence, Coriolis, and bathymetry. *Journal of Physical Oceanography*, *47*(7), 1843–1871. https://doi.org/10.1175/jpo-d-16-0247.1
Wei, X., Schramkowski, G. P., & Schuttelaars, H. M. (2016). Salt dynamics in well-mixed estuaries: Importance of advection by tides. *Journal of Physical Oceanography*, *46*(5), 1457–1475. https://doi.org/10.1175/jpo-d-15-0045.1
Wei, X., Schuttelaars, H. M., Williams, M. E., Brown, J. M., Thorne, P. D., & Amoudry, L. O. (2021). Unraveling interactions between asymmetric tidal turbulence, residual circulation, and salinity dynamics in short, periodically weakly stratified estuaries. *Journal of Physical Oceanography*, *51*(5), 1395–1416. https://doi.org/10.1175/jpo-d-20-0146.1
Zhu, J., Cheng, X., Li, L., Wu, H., Gu, J., & Lyu, H. (2020). Dynamic mechanism of an extremely severe saltwater intrusion in the Changjiang estuary in February 2014. *Hydrology and Earth System Sciences*, *24*(10), 5043–5056. https://doi.org/10.5194/hess-24-5043-2020

References From the Supporting Information

David, V., Sautour, B., Chardy, P., & Leconte, M. (2005). Long-term changes of the zooplankton variability in a turbid environment: The Gironde estuary (France). *Estuarine, Coastal and Shelf Science*, *64*(2–3), 171–184. https://doi.org/10.1016/j.ecss.2005.01.014
Garvine, R. W., McCarthy, R. K., & Wong, K.-C. (1992). The axial salinity distribution in the Delaware estuary and its weak response to river discharge. *Estuarine, Coastal and Shelf Science*, *35*(2), 157–165. https://doi.org/10.1016/s0272-7714(05)80110-6
Naithani, J., de Brye, B., Buyze, E., Vyverman, W., Legat, V., & Deleersnijder, E. (2016). An ecological model for the Scheldt estuary and tidal rivers ecosystem: Spatial and temporal variability of plankton. *Hydrobiologia*, *775*(1), 51–67. https://doi.org/10.1007/s10750-016-2710-1

Sharp, J. H., Yoshiyama, K., Parker, A. E., Schwartz, M. C., Curless, S. E., Beauregard, A. Y., et al. (2009). A biogeochemical view of estuarine eutrophication: Seasonal and spatial trends and correlations in the Delaware estuary. *Estuaries and Coasts*, *32*(6), 1023–1043. https://doi.org/10.1007/s12237-009-9210-8

Uncles, R., & Stephens, J. (1993). The freshwater-saltwater interface and its relationship to the turbidity maximum in the Tamar estuary, United Kingdom. *Estuaries*, *16*(1), 126–141. https://doi.org/10.2307/1352770

van Maanen, B., & Sottolichio, A. (2018). Hydro- and sediment dynamics in the Gironde estuary (France): Sensitivity to seasonal variations in river inflow and sea level rise. *Continental Shelf Research*, *165*, 37–50. https://doi.org/10.1016/j.csr.2018.06.001